Net Methylation of Mercury in Estuarine Sediment Microcosms Amended with Dissolved, Nanoparticulate, and Microparticulate Mercuric Sulfides

ARTICLE *in* ENVIRONMENTAL SCIENCE AND TECHNOLOGY · JULY 2014

Impact Factor: 5.33 · DOI: 10.1021/es500336j · Source: PubMed

5 AUTHORS, INCLUDING:

Tong Zhang
Woods Hole Oceanographic Institution
10 PUBLICATIONS **281** CITATIONS
SEE PROFILE

Katarzyna (Kate) H Kucharzyk
Battelle Memorial Institute
14 PUBLICATIONS **163** CITATIONS
SEE PROFILE

Marc Deshusses
Duke University
151 PUBLICATIONS **4,934** CITATIONS
SEE PROFILE

Environmental Science & Technology

Article

pubs.acs.org/est

Net Methylation of Mercury in Estuarine Sediment Microcosms Amended with Dissolved, Nanoparticulate, and Microparticulate Mercuric Sulfides

Tong Zhang,[†,§] Katarzyna H. Kucharzyk,[†] Bojeong Kim,[‡,∥] Marc A. Deshusses,[†] and Heileen Hsu-Kim*[,†]

[†]Duke University, Department of Civil and Environmental Engineering, 121 Hudson Hall, Durham, North Carolina 27708 United States

[‡]Virginia Polytechnic Institute and State University, Department of Geosciences, Blacksburg, Virginia 24061 United States

[§]Woods Hole Oceanographic Institution, Department of Marine Chemistry and Geochemistry, 266 Woods Hole Road, Woods Hole, Massachusetts 02543 United States

[∥]Temple University, Department of Earth and Environmental Science, Philadelphia, Pennsylvania 19122 United States

Supporting Information

ABSTRACT: The production of methylmercury (MeHg) by anaerobic microorganisms depends in part on the speciation and bioavailability of inorganic mercury to these organisms. Our previous work with pure cultures of methylating bacteria has demonstrated that the methylation potential of mercury decreased during the aging of mercuric sulfides (from dissolved to nanoparticulate and microcrystalline HgS). The objective of this study was to understand the relationship between mercury sulfide speciation and methylation potential in experiments that more closely simulate the complexity of sediment settings. The study involved sediment slurry microcosms that represented a spectrum of salinities in an estuary and were each amended with different forms of mercuric sulfides: dissolved Hg and sulfide, nanoparticulate HgS (3−4 nm in diameter), and microparticulate HgS (>500 nm). The results indicated that net MeHg production was influenced by both the activity of sulfate-reducing microorganisms (roughly represented by the rate of sulfate loss) and the bioavailability of mercury. In the presence of abundant sulfate and carbon sources (supporting relatively high microbial activity), net MeHg production in the slurries amended with dissolved Hg was greater than in slurries amended with nano-HgS, similar to previous experiments with pure bacterial cultures. In microcosms with minimal microbial activity (indicated by low rates of sulfate loss), the addition of either dissolved Hg or nano-HgS resulted in similar amounts of net MeHg production. For all slurries receiving micro-HgS, MeHg production did not exceed abiotic controls. In slurries amended with dissolved and nano-HgS, mercury was mainly partitioned to bulk-scale mineral particles and colloids, indicating that Hg bioavailability was not simply related to dissolved Hg concentration or speciation. Overall, the results suggest that models for mercury methylation potential in the environment will need to balance the relative contributions of mercury speciation and activity of methylating microorganisms.

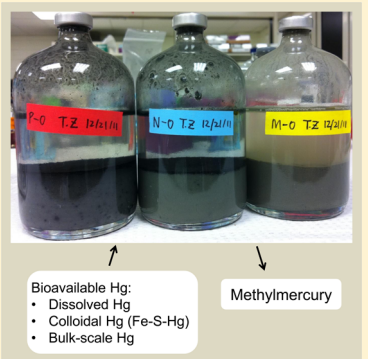

INTRODUCTION

Methylmercury (MeHg) is a neurotoxin that is produced in aquatic ecosystems mainly through anaerobic microorganisms that are abundant in sediments and other settings.[1,2] The production rate of MeHg can vary across aquatic ecosystems, sometimes by orders of magnitude.[3−5] Although numerous studies have been conducted to investigate the microbiological[6−9] and geochemical factors[10−14] that control MeHg production in natural sediments, great uncertainty remains regarding the biochemical pathway of MeHg production and the identity of inorganic mercury species that are available to microorganisms for methylation.[15] Moreover, it is not known how one factor can be more important than others for controlling mercury methylation.

Our previous studies[16,17] indicated that the bioavailability of mercury for methylation decreased during the aging of mercuric sulfides in anaerobic settings, a process in which mercury is expected to comprise a mixture of dissolved, nanoparticulate, and microparticulate forms of Hg-sulfides that represent different reaction products during the precipitation and dissolution of HgS. Our results demonstrated that when sulfate reducing bacteria (SRB) *Desulfobulbus propionicus* and *Desulfovibrio desulfuricans* were exposed to nanoparticulate HgS, the cultures produced MeHg at significantly higher rates relative to cultures receiving microcrystalline HgS. Dissolved mercury concentration (i.e., mercury that passed through 0.02 μm filters or remained in the supernatant after ultracentrifugation) was able to explain some, but not all, of the

Received: January 21, 2014
Revised: July 2, 2014
Accepted: July 9, 2014

   dx.doi.org/10.1021/es500336j | Environ. Sci. Technol. XXXX, XXX, XXX−XXX

differences in methylation by the pure cultures grown under fermentative conditions.

While this previous work highlighted the importance of Hg-sulfide speciation for MeHg production and the previously unrecognized role for nanoparticles, natural sediments are much more complex than pure bacterial cultures in aqueous media. For example, natural sediments contain a diverse group of microorganisms that can simultaneously generate and degrade MeHg.[18−20] Nonmethylating microorganisms may also compete with methylating bacteria for nutrients, possibly resulting in limitations to MeHg production rates. The geochemistry of mercury in sediments is also much more complex than can be tested in pure culture experiments. Sediments consist of a mixture of mineral particles, some coated with natural organic matter, that can scavenge mercury from pore water via adsorption, complexation, and aggregation.[21−23] Therefore, results from pure culture studies may not directly apply to real sediments. Thus, it is relevant to examine the aging effect of HgS on mercury bioavailability under more environmentally relevant conditions.

In this study, we conducted sediment slurry microcosm experiments to investigate whether the "aging" states of mercuric sulfides is correlated with net MeHg production, as we observed in pure cultures of SRB. We also sought to understand how environmental variables (e.g., salinity) could influence the partitioning of mercury between various phases (e.g., dissolved, nanoparticulate, microparticulate), growth of methylating microorganisms, and the consequence of these changes for MeHg production. The microcosms were constructed with sediments and water collected at three locations in the San Francisco Bay-Delta estuary (California, U.S.A.) to represent sediment conditions ranging from freshwater to brackish settings. The slurries were amended with one of three forms of mercury: dissolved $Hg(NO_3)_2$ and Na_2S, HgS nanoparticles (3−4 nm in diameter), and HgS microparticles (>500 nm). The slurry experiments were performed twice under variable microbial growth conditions: with added pyruvate as a carbon and energy substrate and without additional carbon. We compared net MeHg production and other water quality parameters relevant for microbial activity and mercury speciation.

MATERIALS AND METHODS

Sediment and Water Collection. Sediment samples were collected in August 2011 as part of the biennial sediment survey conducted by the San Francisco Estuary Institute (SFEI) for their Regional Monitoring Program. Site 1 (BG30, based on SFEI's site identification number) is a freshwater location in the San Joaquin River (38.023° N, 121.808° W). Site 2 (SU044S, 38.076° N, 122.057° W) is located in Suisun Bay, connecting the confluence of the Sacramento and San Joaquin Rivers to San Pablo Bay. Site 3 (LSB129S) is a brackish water location at the southern section of the San Francisco Bay area near the city of San Jose (37.487° N, 122.101° W). Triplicate samples were collected with Van Veen samplers and the top layer (approximately 5 cm) of the sediment was packed into acid-cleaned polyethylene jars with Teflon-lined caps. The sediment samples were covered with a thin layer of overlaying water from the site, and the sample jars were sealed with no headspace. At the same sampling sites, surface water was also collected using acid-cleaned polyethylene jugs filled to capacity. Sediment and water samples were transported on ice to the laboratory at Duke University and stored at 4 °C. The sediments were stirred for a few minutes to homogenize and a portion of each sediment samples was analyzed for total mercury, MeHg, acid volatile sulfide (AVS), and water content. Surface water samples were analyzed for pH, total organic carbon (TOC), sulfate (SO_4^{2-}), ferrous iron (Fe(II)), total Fe, and total mercury content. Procedures for all chemical analyses are described in the Supporting Information.

Pore Water Characterization. Pore waters, as defined for this study, were extracted from the samples by centrifuging the sediments at 3000 *g* for 20 min. The supernatant was analyzed for total mercury concentration and pH. Aliquots for analysis of AVS were preserved with 0.01 N zinc sulfate ($ZnSO_4$) and 0.01 N potassium hydroxide (KOH, trace metal grade), and stored at 4 °C. Pore water samples were also filtered through 0.2 μm nylon syringe filters in an anaerobic chamber and analyzed for Hg, TOC, SO_4^{2-}, Fe(II), and total Fe concentrations.

Hg Fractionation in Pore Water. Particulate, colloidal, and dissolved mercury in pore waters were quantified by fractionating the pore water samples using centrifugation and ultracentrifugation.[16] In summary, we defined bulk particulate fraction as the mercury species that settled from the water after centrifugation at 6700 *g* for 5 min. The mercury in the supernatant was further fractionated by ultracentrifugation at 370000 *g* for 1 h. After ultracentrifugation, the mercury remaining in the supernatant was considered to be nominally dissolved, while mercury in the pellet after ultracentrifugation was operationally defined as colloidal mercury (including nanoparticulate HgS). The ability of this procedure to approximate size fractionation was tested and verified with solutions that comprised either dissolved Hg, nanoparticulate HgS, or microparticulate HgS (Supporting Information, Figure S1a).

HgS Particle Preparation. Stock solutions/suspensions of $Hg(NO_3)_2$, Na_2S, and HgS nanoparticles and microparticulate HgS were prepared according to Zhang et al.[16] and summarized in the Supporting Information. The nano-HgS stock suspension was allowed to age for 16 h at room temperature prior to use in the methylation experiments. Our previous study[16] indicated that the nanoparticulate HgS comprised primarily of metacinnabar-like particles with an average diameter of 3.2 ± 0.8 nm (based on transmission electron microscopy, TEM) and geometric surface area of 264 ± 72 $m^2\ g^{-1}$. The microparticulate HgS was a mixture of metacinnabar and cinnabar particles (based on X-ray diffraction) with an average diameter of 530 ± 367 nm (based on TEM) and geometric surface area of 2.5 ± 1.8 $m^2\ g^{-1}$.

Sediment Slurry Preparation. For slurry preparation, sediments were stirred to homogenize the samples, apportioned into 200 mL acid-cleaned serum bottles, and mixed with the N_2-purged surface water sample obtained from the same site (see Table 1 for details). A redox indicator, resazurin, was added to a final concentration of 2 mg/L. The serum bottles were then capped with butyl rubber stoppers and crimped with aluminum seals. The slurries were preincubated in the dark at room temperature (20−22 °C) to deplete residual oxygen. The slurries were not utilized for mercury methylation experiments until the resazurin became clear (i.e., redox potential < −51 mV). Slurry experiments with sediments from Site 1 and Site 3 were performed two times (experimental conditions summarized in Table 1). These two separate experiments were designed so that microbial growth was more active in Experiment 1 than in Experiment 2. Thus, the procedures differed in the solid-to-water ratio, preincubation period (prior

dx.doi.org/10.1021/es500336j | Environ. Sci. Technol. XXXX, XXX, XXX−XXX

Table 1. Procedures Utilized to Construct Sediment Slurry Microcosm for Two Different Experiments. The Objective Was To Test the Effects of Microbial Activity and Type of Added Mercury on Net Production of Methylmercury

	experiment 1	experiment 2
source of sediment and water	Site 1, Site 2, Site 3	Site 1, Site 3
sediment wet weight	50 g	20 g
water volume	120 mL	140 mL
additional carbon source	10 mM Na–pyruvate[a]	none
preincubation time under anaerobic conditions (prior to Hg addition)	7.5 days	2.5 days
mercury added (as dissolved Hg+S, nano-HgS, and microparticulate HgS)	50 nmol	50 nmol

[a]Na–pyruvate was added to the sediment slurry microcosms prior to the preincubation.

to mercury addition), and external carbon source (added in Experiment 1 only). Sediment from Site 2 was utilized only in Experiment 1.

Mercury Methylation Experiments. After preincubation, sediment slurries were spiked with 50 nmol of mercury as one of the following: dissolved Hg+S (i.e., equimolar amounts of dissolved $Hg(NO_3)_2$ and Na_2S added from their respective stock solutions), HgS nanoparticles, and HgS microparticles. Three sets of controls were also incubated in parallel with the methylation experiments: (1) a blank consisting of sediment slurries without added mercury (i.e., Hg blank); (2) a control slurry amended with 20 mM sodium molybdate, a specific inhibitor of sulfate reduction, added 1 day prior to dosing with dissolved Hg+S (later referred as the molybdate control); (3) a slurry that was autoclaved (121 °C, 30 min) prior to being amended with dissolved Hg+S (later referred as the autoclaved control). In the dissolved Hg+S exposure, the micro-HgS exposure, and the three controls, 10 μg-C of Suwannee River humic acid (International Humic Substances Society), 0.1 mmol of $NaNO_3$, and 4 μmol of sodium 4-(2-hydroxyethyl) piperazine-1-ethanesulfonate (HEPES) were added to the slurries to account for the chemical carryover from the HgS nanoparticle stock in the nano-HgS treatment. After the addition of mercury, all the slurry microcosms were incubated statically for up to 7 days in the dark at room temperature (20–22 °C). The change in MeHg concentration in the microcosms represented the simultaneous production and degradation of MeHg by the cultures. Thus, the term "net MeHg production" was used to represent these processes.

Experiments 1 and 2 lasted 7.1 and 2.8 days, respectively, during which replicate serum bottles (n = 2–3) were sacrificed periodically for chemical and biological analyses. At the time of sample collection, the slurries were first mixed once end-over-end and allowed to settle for 10 min. Then, 1 mL of gas was collected from the headspace using a gastight syringe. The gaseous mercury content (e.g., Hg^0, dimethylmercury) in these samples was analyzed by injecting the sample into a gastight vial filled with ultrapure water (Barnstead Nanopure, >18 MΩ-cm) containing 2% (v/v) BrCl. These samples were stored and equilibrated for at least 3 days at room temperature prior to total mercury analysis in the liquid.

After collection of the headspace sample, liquid aliquots were withdrawn from the water overlaying the sediment, filtered through 0.2 μm nylon syringe filters and preserved for chemical analysis, including total Hg, AVS, TOC, major anions (e.g., SO_4^{2-} and Cl^-) and major cations concentrations. A drop of the 0.2-μm filtered water samples was placed on a 200-mesh copper TEM grid with lacey carbon support film (Electron Microscopy Sciences, PA) and then allowed to evaporate in an anaerobic chamber (Coy Lab Products). The samples were later analyzed by a FEI Titan 80-300 field emission TEM operated at 200 keV and equipped with an energy dispersive X-ray (EDX) spectrometer for chemical analysis. pH and dissolved Fe(II) concentration were also measured immediately after collection of these liquid samples. Aliquots of the sediment–water mixture were fractionated using the (ultra)-centrifugation method (as described in the previous section "Hg fractionation in pore water") to separate particulate, colloidal, and dissolved forms of Hg. The remainder of the slurries were frozen (−80 °C) until extraction for DNA and analysis for MeHg and total mercury content. All sample collection operations were conducted in an anaerobic chamber.

Equilibrium Speciation Calculations. Dissolved phase Hg speciation for Site 3 slurries in Experiment 1 was estimated using equilibrium speciation models, as detailed in the Supporting Information. The calculations utilized the measured Hg concentration in ultracentrifuged pore water samples and the measured pH, Fe(II), AVS, Cl^-, and thiol concentrations in filtered (<0.2 μm) pore water samples. The calculations did not incorporate equilibration with solids.

Saturation indices for metacinnabar, mackinawite, and pyrite were also calculated using concentration data of the 0.2 μm-filtered fractions. These calculations were used to assess the potential presence of colloidal metal sulfides.

RESULTS AND DISCUSSION

Sediment and Pore Water Characteristics. The composition of samples from the three sites represented a typical gradient found in an estuarine setting (Table 2), in which salinity varied from 0.46 to 24 psu and dissolved SO_4^{2-} concentration varied from 0.69 to 22 mM in surface water. Total Hg contents were relatively low in both sediment (190–1900 pmol g^{-1}) and pore water (150–690 pmol L^{-1}) samples and fell within the range of previous measurements for the San Francisco Bay-Delta region.[24] Total Fe was detected at 0.018 to 0.27 mM in pore waters, with Fe(II) representing 83% and 52% of total Fe at Site 1 and Site 3. Fe(II) concentration in sediment pore water from Site 2 was below the detection limit. Size fractionation of mercury in sediment pore water by centrifugation revealed that the majority of the mercury in suspension was associated with bulk-scale particles (Supporting Information, Figure S1b).

Net MeHg Production in Sediment Slurry Microcosms. Net production of MeHg in the microcosm experiments was, for the most part, dependent on the type of mercury added (i.e., dissolved, nanoparticulate, microparticulate) (Figure 1 and Supporting Information, Figure S2). Other water quality parameters such as pH and dissolved Fe and AVS concentrations did not depend on the type of mercury sulfide added (Figures S3–S5). These results are consistent with our previous study with pure culture.[16] In Experiment 1, which involved a carbon amendment to promote anaerobic growth, the three forms of mercury were added at a concentration (2 nmol g^{-1}(dw)) that corresponded to 1.0, 10.6, and 1.4 times the concentration of the ambient total mercury in sediments from Site 1, Site 2, and Site 3, respectively (Table 2). The resulting MeHg concentration at the end of the experiment in dissolved and nano-HgS amended slurries was 17 to 1400 times

dx.doi.org/10.1021/es500336j | Environ. Sci. Technol. XXXX, XXX, XXX–XXX

Table 2. Characteristics of Sediment Pore Water, Whole Sediment, and Surface Water Samples Used for Slurry Microcosm Experiments

parameters	sample site		
	Site 1 (BG30)	Site 2 (SU044S)	Site 3 (LSB129S)
	Pore Water[a]		
pH	7.4	7.5	7.7
TOC (mg L^{-1})	20 ± 0.2	9.2 ± 0.3	16 ± 0.1
SO_4^{2-} (mM)	0.40 ± 0.09	9.0 ± 0.7	20 ± 0.5
AVS (μmol L^{-1})	1.0 ± 0.2	11 ± 2	21 ± 4
Fe(II) (mM)	0.10 ± 0.003	<DL[d]	0.14 ± 0.001
total Fe (mM)	0.12 ± 0.002	0.018 ± 0.0004	0.27 ± 0.01
total Hg (pmol L^{-1})	694 ± 134	185 ± 24	147 ± 27
	Whole Sediment[b]		
AVS (μmol g^{-1})	1.3 ± 0.3	8.2 ± 0.9	13 ± 2
total Hg (pmol g^{-1})	1943 ± 104	188 ± 14	1477 ± 57
MeHg (pmol g^{-1})	2.2 ± 0.6	1.6 ± 0.3	13 ± 1
	Surface Water[c]		
salinity (psu)[e]	0.46 ± 0.03	7.0 ± 0.03	24 ± 0.1
pH	7.6	7.7	7.9
TOC (mg L^{-1})	2.8 ± 0.3	4.0 ± 0.2	4.1 ± 0.1
SO_4^{2-} (mM)	0.69 ± 0.01	8.9 ± 0.3	22 ± 0.05
Fe(II) (mM)	<DL[d]	<DL[d]	<DL[d]
total Fe (mM)	0.0055 ± 0.0001	0.0090 ± 0.0003	0.011 ± 0.0003
total Hg (pmol L^{-1})	0.020 ± 0.006	0.017 ± 0.006	0.011 ± 0.0005

[a]Pore water was collected from the supernatant of whole sediment samples that were centrifuged at 3000 *g* for 20 min. The values represent mean ± standard deviation of triplicate samples. [b]The values represent mean ± standard deviation of triplicate samples and are expressed on a dry weight (dw) basis. [c]The values represent the mean and the range of duplicate samples. [d]<DL: values below the detection limit of Fe(II), 0.004 mM. [e]The salinity data were provided by the Regional Monitoring Program at the San Francisco Estuary Institute.

and 16 to 364 times greater than the "Hg blank" (i.e., slurries without Hg addition and only containing Hg species from the original sediment, Figure 1). In slurries amended with microparticulate HgS, net production of MeHg was minimal and similar to the Hg blank (Figure 1). These observations indicate that more "aged" forms of mercury (i.e., microcrystalline HgS, native Hg in the sediments) had lower potential to be methylated compared to newer forms of Hg such as recently deposited dissolved Hg and freshly precipitated or adsorbed particulate Hg.

In the Site 2 and Site 3 slurry samples for Experiment 1, higher net MeHg production was obtained from slurries amended with dissolved $Hg(NO_3)_2$ and Na_2S than slurries amended with nano-HgS. (Figure 1b and 1c). This trend did not appear in the sediment slurry for Site 1 (Figure 1a): no difference in net MeHg production was observed between microcosms amended with dissolved Hg+S and nano-HgS. The comparisons between dissolved Hg+S and nano-HgS amendments were explored further by investigating how microbial activity could be controlling net MeHg production.

Sulfate reducing bacteria (SRB) appeared to be the primary methylators of mercury in these microcosms, as indicated by experiments performed with the addition of molybdate, a specific metabolic inhibitor of SRB. In slurries treated with molybdate, the concentrations of MeHg at the end of the incubation for Site 1, Site 2, and Site 3 were 7.1 ± 0.6%, 2.1 ± 0.1%, and 7.3 ± 1.1%, respectively, of MeHg in slurries without molybdate but amended with the same type of mercury (i.e., dissolved Hg+S) (Figure 1). This result is consistent with the dominant role of SRB for the production of MeHg, as demonstrated by many other studies.[2,25−27]

The number of the sulfite reductase *dsr*A gene copies and the abundance of *dsr*A relative to 16s rRNA genes in the slurry microcosms remained largely the same in the three different mercury treatments (Supporting Information, Figure S6). This result indicates that the difference in MeHg production (Figure 1) could not be explained by the abundance of SRB as determined by the prevalence of *dsr*A genes, even though molybdate inhibition suggested the importance of sulfate reducers for mercury methylation. This discrepancy may be due to a poor correlation of the *dsr*A gene with SRB activity and with net MeHg production for these microcosm experiments.

The activity of SRB was roughly approximated by the rate of sulfate loss during the incubation. In the slurry samples with relatively high initial sulfate concentrations (i.e., Site 2 and Site 3), rates of sulfate loss were at least 0.2 mM d^{-1} and relatively similar in all mercury sulfide exposures (Supporting Information, Figure S7b and S7c and Table S2). Mercury methylation in these microcosms was most likely controlled by the speciation and bioavailability of inorganic mercury. However, in the low sulfate slurries (i.e., Site 1), sulfate was nearly completely consumed (i.e., close to the 0.01 mM detection limit) after the 7.5-day preincubation prior to Hg addition (Supporting Information, Figure S7a). The rate of sulfate loss during Hg methylation was less than 0.01 mM d^{-1}. Microbial activity in the Site 1 microcosms was likely a limiting factor for MeHg production, particularly in the presence of abundant bioavailable mercury species (i.e., slurries treated with dissolved and nano-HgS, Figure 1a).

In addition to sulfate abundance, net MeHg production also appeared to be affected by the availability of organic carbon. In Site 3 slurries, where sulfate was abundant, net MeHg production was enhanced by the addition of pyruvate in Experiment 1 relative to Experiment 2 with no pyruvate (Figure 1c and Supporting Information, Figure S2b). The average rates of net MeHg production for the dissolved HgS and nano-HgS treatments within the first 3 days of incubation was 2.58 ± 0.51 pmol g^{-1} h^{-1} and 0.68 ± 0.53 pmol g^{-1} h^{-1} in Experiment 1, and 0.22 ± 0.06 pmol g^{-1} h^{-1} and 0.24 ± 0.0005 pmol g^{-1} h^{-1} in Experiment 2, respectively. Despite the higher inorganic mercury loading per sediment mass, net MeHg production in Experiment 2 was apparently limited by the bacterial activity, indicated by the minimal sulfate loss (Supporting Information, Figure S8). The availability of labile organic carbon for microbial metabolism is known to be an important factor for microbial MeHg production.[3,9] The addition of pyruvate in Experiment 1 enhanced mercury methylation without significantly affecting the relative abundance of the sedimentary SRB community (the ratio of *dsr*A/16s rRNA remained similar during the 7-day incubation, Figure S6). In Experiment 2, TOC did not appear to decrease during the incubation (Figure S9), possibly due to the limited bioavailability of the native organic carbon for microbial metabolism.

Mercury Fractionation, Speciation, And Methylation Potential in Sediment Slurry Microcosms. The microcosm experiments demonstrated that in most cases, net production of MeHg depended on the type of mercury added. To further

dx.doi.org/10.1021/es500336j | Environ. Sci. Technol. XXXX, XXX, XXX−XXX

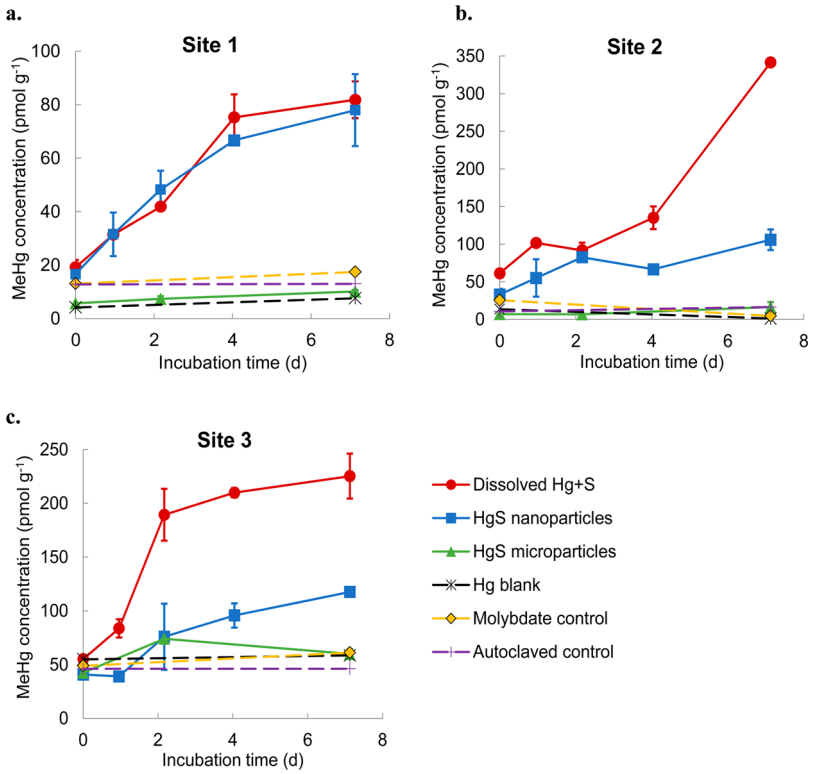

Figure 1. Net MeHg production in the slurry microcosms after the addition of 2 nmol Hg g^{-1} (dw sediment) in the form of dissolved $Hg(NO_3)_2$ and Na_2S, HgS nanoparticles or HgS microparticles in Experiment 1. The slurries were prepared with sediments from (a) Site 1, (b) Site 2, and (c) Site 3. The MeHg concentration was normalized to the dry sediment mass in each serum bottle. Incubation time represents the time after Hg amendments. The error bars represent the range of duplicate samples in the test groups. Single replicate of slurries were incubated for the controls. The "Hg blank" consisted of sediment slurries without added mercury. The "Molybdate control" and "Autoclaved control" were amended with dissolved $Hg(NO_3)_2$ and Na_2S.

explore the relationship between mercury speciation and its methylation potential, mercury in the Site 1 and Site 3 slurries in Experiment 1 was quantified in different fractions of the microcosms. The highest concentration of Hg detected in the headspace of these samples accounted for <0.1% of total Hg spiked in the microcosms. Hence, the production of gaseous Hg was not significant in our experiments.

Fractionation of the pore waters using sequential centrifugation indicated that the nominally dissolved mercury contents in the slurries amended with dissolved Hg+S and nano-HgS were larger than dissolved mercury in micro-HgS amended slurries and the "Hg blank" (Figure 2). However, more than 98% of the added Hg partitioned into the bulk particulate fraction within 15 min of addition (regardless of the type of mercury added). In our previous research with pure cultures, the concentration of dissolved Hg (defined by the same approach) was consistent with trends in MeHg production.[16] Thus, the higher concentration of dissolved Hg may explain the greater amount of net MeHg production in slurries that were amended with dissolved and nano-HgS relative to the other slurries (Figure 1).

However, in the microcosm experiments, the dissolved Hg fraction alone did not explain the MeHg production in Site 3 slurries amended with dissolved Hg+S and HgS nanoparticles. In these samples, the dissolved Hg contents and speciation were similar in the two mercury exposures (Figure 2c,d, and Supporting Information, Figure S10), while net MeHg production differed significantly (Figure 1c). Previous researchers have hypothesized that neutrally charged Hg species represent the bioavailable forms of Hg.[3,28] However, for Site 3 slurries, the sum of the concentrations of neutral Hg complexes in the dissolved Hg+S treatment did not exceed that in the nano-HgS treatment (Figure S11), a pattern that is inconsistent with the trend in net MeHg production (Figure 1c). The discrepancy is probably caused by the bulk-scale sedimentary particles in the microcosms. The majority of the mercury added as dissolved Hg or nanoparticles was not observed in the dissolved or colloidal phase of the slurry microcosms (only 0.3−1.3% of the added mercury remained in the supernatant after centrifugation at 6700 *g* for 5 min) and probably sorbed to or deposited onto large particles and microorganisms in the slurries.

Microorganisms tend to attach to the surface of mineral particles via sorption or biofilm formation.[29] Hence, sedimentary particles are the likely sites of MeHg production. Indeed, solid-phase dissolution and surface desorption of inorganic Hg has been proposed to control Hg bioavailability in sediments,[23] and bioavailability will increase in scenarios where weakly sorbed or highly soluble particulate Hg species closely associate with sites of methylation.

The relative amounts of dissolved and colloidal mercury in the microcosms depended on the type of sediment and salinity. A substantial amount of colloidal mercury was detected in Site 1 slurries (the freshwater site) amended with dissolved Hg+S and nano-HgS, and this colloidal fraction increased during the 7-day incubation period (Figure 2a,b). In contrast, the colloidal mercury concentration in the Site 3 slurries (the brackish water site) was less than the dissolved fraction and decreased to

dx.doi.org/10.1021/es500336j | *Environ. Sci. Technol.* XXXX, XXX, XXX−XXX

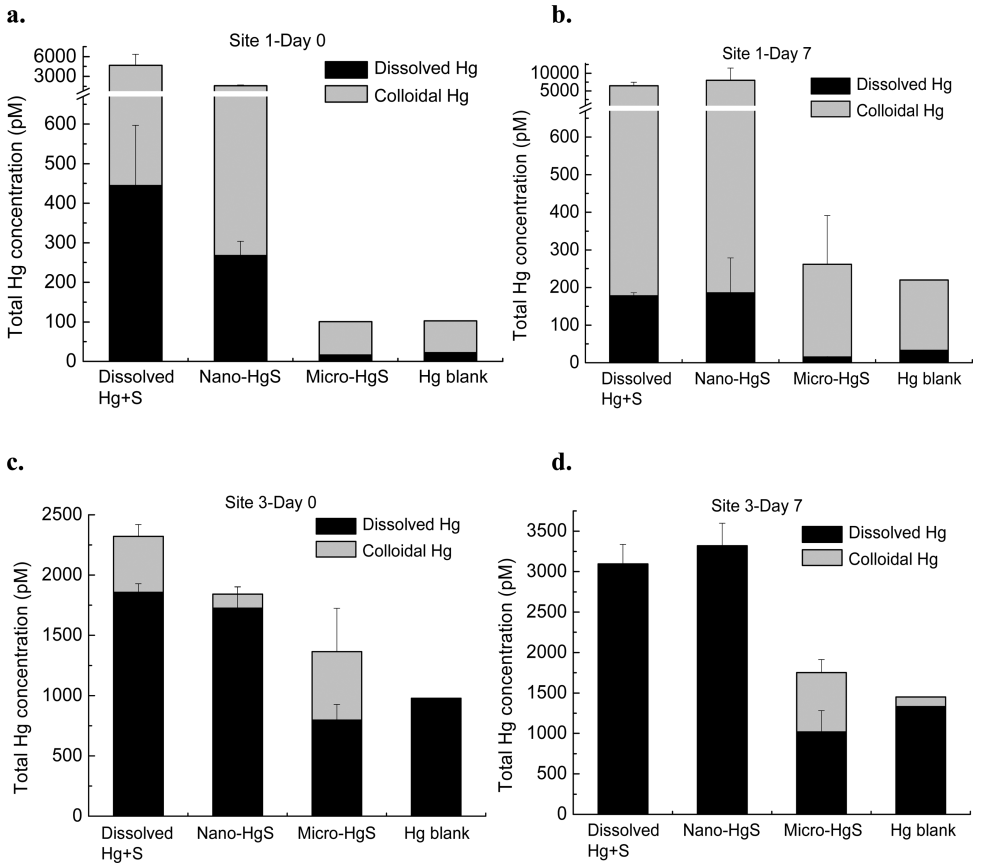

Figure 2. Hg fractionation in sediment slurries amended with 2 nmol g^{-1} (dw sediment) added as dissolved $Hg(NO_3)_2$ and Na_2S, HgS nanoparticles or HgS microparticles in Experiment 1. This Hg spike corresponded to 345 nmol Hg per L of water was added into the slurries. The slurries were prepared with sediments from Site 1 (a and b) and Site 3 (c and d). (Ultra) centrifugation was performed within 15 min (a and c) and 7 days (b and d) after mercury amendments. "Dissolved Hg" represents the total Hg that remained in the supernatant after ultracentrifugation at 370 000 *g* for 1 h. "Colloidal Hg" represents the concentration difference of supernatant Hg after centrifugation at 6700 *g* for 5 min and ultracentrifugation at 370 000 *g* for 1 h. "Hg blank" represents slurries without mercury addition. The error bars represent the range of duplicate samples in the test groups. Single replicates of slurries were incubated for the Hg blank control.

undetectable levels after 7 days (Figure 2c,d). These results suggest that dispersed HgS nanoparticles may exist for a relatively long time in the pore water of freshwater settings, likely via stabilization by natural organic matter,[30] and perhaps produce a source of mercury for microbial methylation. In high salinity waters, these nanoparticles are subject to aggregation and partitioning to the larger particle fraction.

Potential Influence of Iron Sulfide Minerals. In sedimentary environments, other sulfide-complexing metals, such as Zn, Fe, and Cu, often coexist at much higher levels relative to Hg. In particular, due to the high abundance of iron in pore waters, Fe(II) likely controls the sulfide speciation and thus indirectly influences the speciation and bioavailability of inorganic Hg. In sediment pore waters from Site 1 and Site 3, Fe(II) was detected at micromolar quantities (Table 2). Also, we observed a black layer on the sediment surface of the Site 3 slurry microcosms, indicative of FeS precipitates.

Equilibrium calculations were performed for the 0.2 μm-filtered fraction to evaluate whether metal sulfide precipitation was thermodynamically possible. The solubility product K_{s0} for metacinnabar ($HgS_{(s)} + H^+ = Hg^{2+} + HS^-$) varies by 4 orders of magnitude in a database of critically selected stability constants.[31] Here, we utilized two values at the high and low end of this range (10^{-36} and 10^{-40}) for our calculations.

The results of the calculations indicated that the precipitation of metal sulfide particles, including metacinnabar, pyrite, and mackinawite was thermodynamically favored in the 0.2 μm-filtered fraction of most microcosms (Figure 3). For the Site 1 slurries, the speciation calculations indicated that the $HgS_{(s)}$ saturation index (defined by log Q/K_{s0}) was greater than zero in slurries treated with dissolved Hg+S and nano-HgS for both values of K_{s0} (Figure 3a,b). This result indicated that $HgS_{(s)}$ was above saturation, and precipitation of metacinnabar was thermodynamically favored in these filtered samples. In the Site 1 slurries amended with micro-HgS or no Hg (i.e., Hg blank), oversaturation of $HgS_{(s)}$ could also occur, particularly at the end of the incubation (Figure 3b). Nanoparticles are small enough to pass through the 0.2-μm filters, although a portion may adsorb or deposit on the filter membrane surface. These calculations point to the possibility that nanoparticulate mercury species existed in the pore water of Site 1 slurry microcosms, consistent with our observations in the fractionation data (Figure 2a,b). In contrast, the speciation calculations indicated smaller (negative, if $K_{s0} = 10^{-36}$) saturation indices of metacinnabar in Site 3 samples (Figure 3c,d), suggesting a lower thermodynamic driving force for HgS precipitation and particle formation.

The saturation indices for pyrite were +10 to +11 in all the samples (Figure 3), indicating a high potential for $FeS_{2(s)}$

dx.doi.org/10.1021/es500336j | Environ. Sci. Technol. XXXX, XXX, XXX–XXX

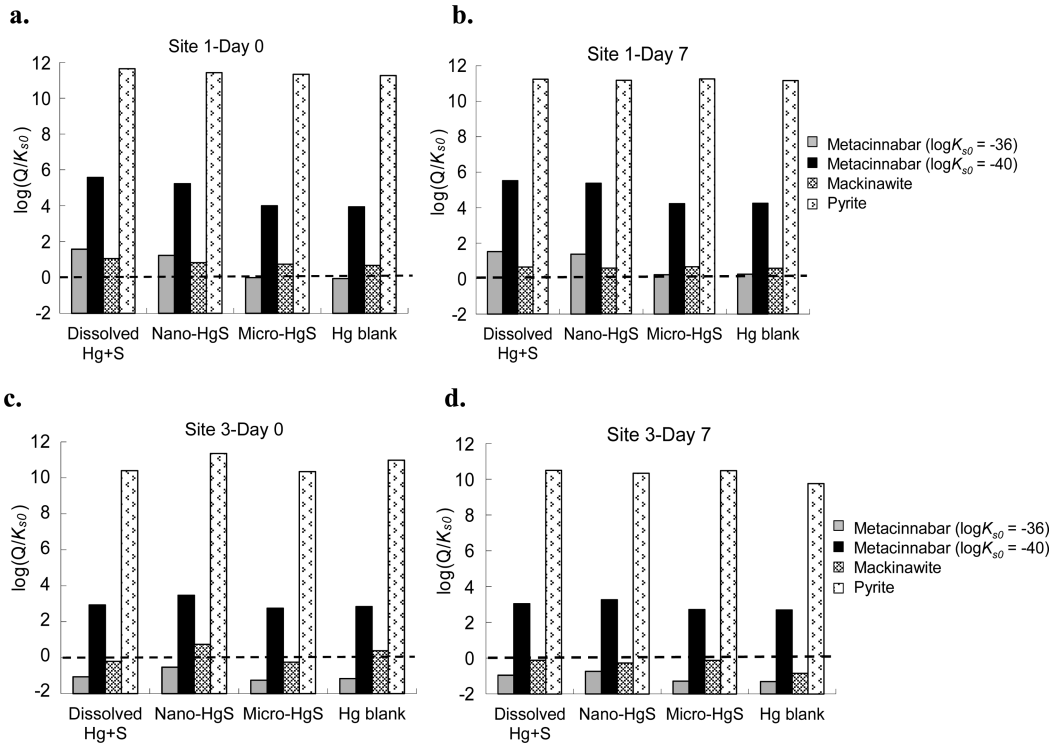

Figure 3. Calculated saturation indices for 0.2-μm filtered water samples withdrawn from the sediment slurries amended with 2 nmol g^{-1} (dw sediment) dissolved $Hg(NO_3)_2$ and Na_2S, HgS nanoparticles or HgS microparticles in Experiment 1. The slurries were prepared with sediments from Site 1 (a and b) and Site 3 (c and d). Saturation indices of metacinnabar (β-$HgS_{(s)}$), mackinawite ($FeS_{(s)}$) and pyrite ($FeS_{2(s)}$) were calculated using measured pH, Hg, Fe(II), AVS, Cl^-, and DOC concentrations in 0.2-μm filtered water samples collected at two time points during the methylation experiments: (a and c) immediately (less than 10 min) and (b and d) 7 days.

formation if S^0 was present in the sediments. Moreover, all Site 1 samples were oversaturated with respect to mackinawite, while the saturation indices of $FeS_{(s)}$ were near or below zero in most Site 3 samples.

Examination of the slurry samples with TEM revealed that amorphous nanoscale particles were present in the 0.2-μm filtered water from the Site 1 slurry microcosms amended with dissolved and nano-HgS (Supporting Information, Figure S12a,b). According to the EDX analysis, these nanoparticles mainly contained Fe and S (Figure S12c,d). Although the mercury concentration in these 0.2-μm filtered water samples was too low to be detected by TEM-EDX, these results suggested that the colloidal mercury fraction in the slurry samples (Figure 2a,b) could be associated with FeS via aggregation, adsorption to or coprecipitation with FeS nanoparticles.[32,33] A recent study with estuarine sediments has demonstrated that mercury associated with mackinawite has a greater methylation potential compared to metacinnabar and cinnabar.[23] Therefore, colloidal HgS/FeS species may play an important role in microbial mercury methylation, especially at settings where sulfate and iron reducing bacteria coexist.[34]

Environmental Implications. The results of the slurry microcosm experiments supported the major observation from our previous study with pure cultures:[16] the aging of mercury (from dissolved Hg to nanoparticulate HgS and then crystalline micro-HgS) decreased the bioavailability of mercury for microbial methylation. The microcosms also provided new insights regarding the complexity of the interconnected relationships between mercury speciation, microbial productivity, and mercury methylation potential. For example, mercury added as dissolved species and as nanoparticulate HgS did not always result in different rates of MeHg production. In these cases, microbial productivity was likely the limiting factor for methylation. Furthermore, most of the dissolved and nanoparticulate species added to the microcosms partitioned to the large particle fraction. Even so, MeHg production was greater in these microcosms than in microcosms receiving microparticulate HgS. This result highlights the weakness in directly relating the "dissolved" fraction (defined by filtration or ultracentrifugation techniques) to methylation potential. Instead, consideration should be given to the chemical reactivity of mercury that is weakly sorbed to mineral particles or composed of nanostructured particles that may fall in the colloidal or large particle fraction.

Results from the slurry microcosm experiments also indicated the importance of nanoscale FeS as the potential carrier of inorganic mercury (as a sorbent for Hg(II) molecules or aggregated with HgS nanoparticles). Previous researchers have proposed the use of Fe(II)-based sediment amendments as a strategy for preventing MeHg accumulation, based on the idea that Fe(II) can reduce the solubility (and subsequent bioavailability) of mercury by decreasing the concentration of dissolved sulfide.[11,35] This result has been demonstrated at high Fe(II) doses but not at low doses of Fe(II).[10,11,35] Perhaps the reason for this inconsistency is that Fe(II) amendments decrease mercury bioavailability by coagulation of colloidal HgS, and low doses of Fe(II) result in a stable occurrence of FeS nanoparticles[36,37] that facilitated mercury bioavailability and methylation. Future research, however, is needed to understand the importance of nano-FeS on microbial mercury methylation.

dx.doi.org/10.1021/es500336j | Environ. Sci. Technol. XXXX, XXX, XXX−XXX

Overall, this study has demonstrated that MeHg production in the sediment microcosms was largely governed by two factors, the productivity of the methylating bacteria and the availability of inorganic mercury. However, under some circumstances one factor appeared to be more important than the other for controlling net methylation rates. Most previous mercury methylation studies[3,4,9,11,18,38,39] have used only actively growing bacteria and/or tested only one type of mercury (typically dissolved Hg) without a full understanding of Hg−sulfide speciation. This study, however, utilized different geochemical conditions (e.g., high and low carbon or sulfate content) and inorganic mercury species with different bioavailability to simultaneously assess the importance of various environmental parameters for MeHg production. Results from this study indicate that the differentiation of factors influencing MeHg production (i.e., mercury bioavailability versus microbial activity) can be achieved by experiments that control for both microbial production and the initial Hg−sulfide speciation. With this approach, measurement methods for mercury bioavailability and methylation potential could be developed and applied toward real environmental settings.

■ ASSOCIATED CONTENT

Supporting Information

Detailed methods for the preparation of HgS nano- and microparticles, chemical analyses, quantitation of total 16S rRNA and *dsrA* gene fragments, method, and stability constants utilized for equilibrium speciation calculations, results of Hg fractionation in sediment pore waters, net MeHg production in Experiment 2, abundance of 16S rRNA and *dsrA* genes, pH, dissolved Fe, AVS, sulfate, and TOC concentrations in the slurry microcosms, modeled dissolved Hg speciation in Site 3 slurries, and the results of TEM-EDX examination of filtered water from Site 1 slurries. This material is available free of charge via the Internet at http://pubs.acs.org.

■ AUTHOR INFORMATION

Corresponding Author

*Phone: (919) 660-5109; fax: (919) 660-5219; e-mail: hsukim@duke.edu.

Notes

The authors declare no competing financial interest.

■ ACKNOWLEDGMENTS

This research was supported by the U.S. Department of Defense Strategic Environmental Research and Development Program (ER-1744) and the U.S. Department of Energy Office of Science Early Career Scientist program (DE-SC0006938). We are grateful to Meg Sedlak, Rachel Allen, and Donald Yee at the San Francisco Estuary Institute and to Paul Salop at Applied Marine Sciences for their assistance with sample site identification and sample collection. We also thank Chuanjia Jiang, Yu-ting (Lusia) Liu, and Brooke Hassett for their assistance with chemical analyses.

■ REFERENCES

(1) Jensen, S.; Jernelov, A. Biological methylation of mercury in aquatic organisms. *Nature* **1969**, *223* (5207), 753−754.

(2) Compeau, G. C.; Bartha, R. Sulfate-reducing bacteria—principal methylators of mercury in anoxic estuarine sediment. *Appl. Environ. Microbiol.* **1985**, *50* (2), 498−502.

(3) Drott, A.; Lambertsson, L.; Bjorn, E.; Skyllberg, U. Importance of dissolved neutral mercury sulfides for methyl mercury production in contaminated sediments. *Environ. Sci. Technol.* **2007**, *41* (7), 2270−2276.

(4) Hintelmann, H.; Keppel-Jones, K.; Evans, R. D. Constants of mercury methylation and demethylation rates in sediments and comparison of tracer and ambient mercury availability. *Environ. Toxicol. Chem.* **2000**, *19* (9), 2204−2211.

(5) Merritt, K. A.; Amirbahman, A. Mercury methylation dynamics in estuarine and coastal marine environments—A critical review. *Earth Sci. Rev.* **2009**, *96* (1−2), 54−66.

(6) Fleming, E. J.; Mack, E. E.; Green, P. G.; Nelson, D. C. Mercury methylation from unexpected sources: Molybdate-inhibited freshwater sediments and an iron-reducing bacterium. *Appl. Environ. Microbiol.* **2006**, *72* (1), 457−464.

(7) Warner, K. A.; Roden, E. E.; Bonzongo, J. C. Microbial mercury transformation in anoxic freshwater sediments under iron-reducing and other electron-accepting conditions. *Environ. Sci. Technol.* **2003**, *37* (10), 2159−2165.

(8) King, J. K.; Kostka, J. E.; Frischer, M. E.; Saunders, F. M.; Jahnke, R. A. A quantitative relationship that demonstrates mercury methylation rates in marine sediments are based on the community composition and activity of sulfate-reducing bacteria. *Environ. Sci. Technol.* **2001**, *35* (12), 2491−2496.

(9) King, J. K.; Kostka, J. E.; Frischer, M. E.; Saunders, F. M. Sulfate-reducing bacteria methylate mercury at variable rates in pure culture and in marine sediments. *Appl. Environ. Microbiol.* **2000**, *66* (6), 2430−2437.

(10) Han, S.; Obraztsova, A.; Pretto, P.; Deheyn, D. D.; Gieskes, J.; Tebo, B. M. Sulfide and iron control on mercury speciation in anoxic estuarine sediment slurries. *Mar. Chem.* **2008**, *111* (3−4), 214−220.

(11) Mehrotra, A. S.; Sedlak, D. L. Decrease in net mercury methylation rates following iron amendment to anoxic wetland sediment slurries. *Environ. Sci. Technol.* **2005**, *39* (8), 2564−2570.

(12) Hammerschmidt, C. R.; Fitzgerald, W. F. Geochemical controls on the production and distribution of methylmercury in near-shore marine sediments. *Environ. Sci. Technol.* **2004**, *38* (5), 1487−1495.

(13) Sunderland, E. M.; Gobas, F.; Branfireun, B. A.; Heyes, A. Environmental controls on the speciation and distribution of mercury in coastal sediments. *Mar. Chem.* **2006**, *102* (1−2), 111−123.

(14) Schartup, A. T.; Mason, R. P.; Balcom, P. H.; Hollweg, T. A.; Chen, C. Y. Methylmercury production in estuarine sediments: Role of organic matter. *Environ. Sci. Technol.* **2013**, *47* (2), 695−700.

(15) Hsu-Kim, H.; Kucharzyk, K. H.; Zhang, T.; Deshusses, M. A. Mechanisms regulating mercury bioavailability for methylating microorganisms in the aquatic environment: A critical review. *Environ. Sci. Technol.* **2013**, *47* (6), 2441−2456.

(16) Zhang, T.; Kim, B.; Leyard, C.; Reinsch, B. C.; Lowry, G. V.; Deshusses, M. A.; Hsu-Kim, H. Methylation of mercury by bacteria exposed to dissolved, nanoparticulate, and microparticulate mercuric sulfides. *Environ. Sci. Technol.* **2012**, *46* (13), 6950−6958.

(17) Pham, A. L.; Morris, A.; Zhang, T.; Ticknor, J.; Levard, C.; Hsu-Kim, H. Precipitation of nanoscale mercuric sulfides in the presence of natural organic matter: Structural properties, aggregation, and biotransformation. *Geochim. Cosmochim. Acta* **2014**, *133*, 204−215.

(18) Bridou, R.; M, M.; Gonzalez, P. R.; Guyoneaud, R.; Amouroux, D. Simultaneous determination of mercury methylation and demethylation capacities of various sulfate-reducing bacteria using species-specific isotopic tracers. *Environ. Toxicol. Chem.* **2011**, *30*, 337−344.

(19) Kerin, E. J.; Gilmour, C. C.; Roden, E.; Suzuki, M. T.; Coates, J. D.; Mason, R. P. Mercury methylation by dissimilatory iron-reducing bacteria. *Appl. Environ. Microbiol.* **2006**, *72* (12), 7919−7921.

(20) Oremland, R. S.; Culbertson, C. W.; Winfrey, M. R. Methylmercury decomposition in sediments and bacterial cultures: Involvement of methanogens and sulfate reducers in oxidative demethylation. *Appl. Environ. Microbiol.* **1991**, *57* (1), 130−137.

(21) Behra, P.; Bonnissel-Gissinger, P.; Alnot, M.; Revel, R.; Ehrhardt, J. J. XPS and XAS study of the sorption of Hg(II) onto pyrite. *Langmuir* **2001**, *17* (13), 3970−3979.

(22) Andrews, J. C. Mercury speciation in the environment using X-ray absorption spectroscopy. *Recent Dev. Mercury Sci.* **2006**, *120*, 1−35.
(23) Jonsson, S.; Skyllberg, U.; Nilsson, M. B.; Westlund, P. O.; Shchukarev, A.; Lundberg, E.; Bjorn, E. Mercury methylation rates for geochemically relevant Hg-II species in sediments. *Environ. Sci. Technol.* **2012**, *46* (21), 11653−11659.
(24) *San Francisco Estuary Institute Regional Monitoring Program dData*; San Francisco Estuary Institute: San Francisco, CA, www.sfei.org (accessed Feb 19,2012).
(25) King, J. K.; Saunders, F. M.; Lee, R. F.; Jahnke, R. A. Coupling mercury methylation rates to sulfate reduction rates in marine sediments. *Environ. Toxicol. Chem.* **1999**, *18* (7), 1362−1369.
(26) Devereux, R.; Winfrey, M. R.; Winfrey, J.; Stahl, D. A. Depth profile of sulfate-reducing bacterial ribosomal RNA and mercury methylation in an estuarine sediment. *Fems Microbiol. Ecol.* **1996**, *20* (1), 23−31.
(27) Gilmour, C. C.; Henry, E. A.; Mitchell, R. Sulfate stimulation of mercury methylation in fresh-water sediments. *Environ. Sci. Technol.* **1992**, *26* (11), 2281−2287.
(28) Benoit, J. M.; Gilmour, C. C.; Mason, R. P.; Heyes, A. Sulfide controls on mercury speciation and bioavailability to methylating bacteria in sediment pore waters. *Environ. Sci. Technol.* **1999**, *33* (6), 951−957.
(29) Long, G. Y.; Zhu, P. T.; Shen, Y.; Tong, M. P. Influence of extracellular polymeric substances (EPS) on deposition kinetics of bacteria. *Environ. Sci. Technol.* **2009**, *43* (7), 2308−2314.
(30) Deonarine, A.; Hsu-Kim, H. Precipitation of mercuric sulfide nanoparticles in NOM-containing water: implications for the natural environment. *Environ. Sci. Technol.* **2009**, *43* (7), 2368−2373.
(31) Smith, R. D.; Martell, A. E. *NIST Critical Stability Constants of Metal Complexes Database*, v. 2.0; NIST: Gaithersburg, MD, 1993.
(32) Jeong, H. Y.; Klaue, B.; Blum, J. D.; Hayes, K. F. Sorption of mercuric ion by synthetic manocrystalline mackinawite (FeS). *Environ. Sci. Technol.* **2007**, *41* (22), 7699−7705.
(33) Morse, J. W.; Luther, G. W. Chemical influences on trace metal−sulfide interactions in anoxic sediments. *Geochim. Cosmochim. Acta* **1999**, *63* (19−20), 3373−3378.
(34) Yu, R. Q.; Flanders, J. R.; Mack, E. E.; Turner, R.; Mirza, M. B.; Barkay, T. Contribution of coexisting sulfate and iron reducing bacteria to methylmercury production in freshwater river sediments. *Environ. Sci. Technol.* **2012**, *46* (5), 2684−2691.
(35) Ulrich, P. D.; Sedlak, D. L. Impact of iron amendment on net methylmercury export from tidal wetland microcosms. *Environ. Sci. Technol.* **2010**, *44* (19), 7659−7665.
(36) Luther, G. W.; Rozan, T. F.; Taillefert, M.; Nuzzio, D. B.; Di Meo, C.; Shank, T. M.; Lutz, R. A.; Cary, S. C. Chemical speciation drives hydrothermal vent ecology. *Nature* **2001**, *410* (6830), 813−816.
(37) Rozan, T. F.; Lassman, M. E.; Ridge, D. P.; Luther, G. W. Evidence for iron, copper, and zinc complexation as multinuclear sulphide clusters in oxic rivers. *Nature* **2000**, *406* (6798), 879−882.
(38) Gilmour, C. C.; Elias, D. A.; Kucken, A. M.; Brown, S. D.; Palumbo, A. V.; C.W, S.; Wall, J. D. Sulfate-reducing bacterium *Desulfovibrio desulfuricans* ND132 as a model for understanding bacterial mercury methylation. *Appl. Environ. Microbiol.* **2011**, *77*, 3938−3951.
(39) Harmon, S. M.; King, J. K.; Gladden, J. B.; Newman, L. A. Using sulfate-amended sediment slurry batch reactors to evaluate mercury methylation. *Arch. Environ. Contam. Toxicol.* **2007**, *52* (3), 326−331.